Journal of Polymer Research (2022) 29: 230
https://doi.org/10.1007/s10965-022-03089-0

ORIGINAL PAPER

Water Hyacinth: A sustainable cellulose source for cellulose nanofiber production and application as recycled paper reinforcement

Meriko Ewnetu Sahlie[1] · Tamene Simachew Zeleke[1] · Fantahun Aklog Yihun[1]

Received: 25 February 2022 / Accepted: 12 May 2022 / Published online: 20 May 2022

Abstract

In this work, cellulose nanofiber was prepared from water hyacinth (WH) using a simple domestic blender and employed as reinforcement in recycled paper. There are various sources to prepare cellulose nanofiber. However, water hyacinth was used as a source to synthesize cellulose in this study to decrease its devastating effect on the water body. Pure cellulose was isolated from water hyacinth with chemical treatments including dilute alkali swelling and bleaching. The chemical composition of water hyacinth was gravimetrically determined and the result demonstrated that cellulose is the largest constituent of the plant (55%), followed by hemicelluloses (19%) and lignin (14%). The remaining 12% was related to other extracts like fat, oil, pectin, etc. As the FTIR data revealed, the functional groups corresponding to lignin and hemicelluloses were absent in the FTIR spectra of extracted cellulose. To increase its functionality, the prepared cellulose was disintegrated into nanofibers using a simple mechanical treatment. To learn more about cellulose fibrillation, UV–Vis spectroscopy was used to analyze the light transmittance of 1 wt% water dispersed, mechanically treated cellulose. The dispersion showed high light transparency, particularly at a higher wavelength. As a result of the cellulose dispersion's reasonable light transmittance value, it can be deduced that the aggregated cellulose chains were efficiently transformed into nanofibers. The inclusion of cellulose nanofibers as reinforcement significantly improved recycled paper's moisture resistance, thermal stability, and mechanical strength.

Keywords Water hyacinth · Cellulose nanofiber · Recycled paper · Thermal properties · Mechanical properties · Nanocomposites

Introduction

Today, with the increasingly serious problems of environmental pollution due to the aggregation of synthetic polymer waste, green biodegradable materials (i.e. cellulose, starch, and protein) have been extensively demanded. Researchers have been urged to utilize biomass materials in various fields, including energy storage and conversion, polymer composites, etc., in different forms, as a result of the increased interest in environmental sustainability and availability [1–3]. Among the biomasses, cellulose is well known as one of the most abundant biodegradable materials in nature [4, 5]. Cellulose is not only the richest biopolymer on earth but also a renewable, biodegradable, carbon–neutral material. Structurally, it is a linear chain of several hundred to many thousands of β (1—4) linked D-glucose units, with a chemical formula of $(C_6H_{10}O_5)_n$. The structure of linear cellulose molecules can be arranged into larger entities with networks through the formation of intra and inter hydrogen bonds, resulting in poor solubility in water and other organic solvents, which has limited its application. One approach for addressing this issue is to use mechanical and chemical treatments to disintegrate bulk cellulose into cellulose nanofibers. Nanofibers are materials that have a diameter of 1–100 nm at least in one dimension and an aspect ratio of greater than 100 [6, 7]. Though the bulk cellulose can be used in many situations, the structure of cellulose at the nanoscale (cellulose nanofibers) can provide extra distinct properties such as high mechanical strength and modulus, large specific surface area, high aspect ratio, environmental benefits, and low coefficient of thermal expansion [8, 9]. Such remarkable properties enabled CNFs to be used in

✉ Fantahun Aklog Yihun
aklogfan@gmail.com

[1] Department of Industrial Chemistry, College of Science, Bahir Dar University, P.O.Box, 79, Bahir Dar, Ethiopia

different industrial applications, such as papermaking, composites, packaging, coatings, bio-medicine, and automotive.

There are various lignocellulose biomasses to prepare cellulose nanofibers like fruits, vegetables, bamboo, rice straw, banana peel, water hyacinth stem, grass, etc. Components such as cellulose, hemicelluloses, lignin, and some extractable portions make up the cell wall structure of these lignocellulosic biomasses. However, most of these lignocellulose biomasses are obtained from seasonable and slow-growing plants and are also utilized for other purposes. Hence, the finding of lignocellulose biomass with fast growth rates, non-seasonable, and less utilized for other purposes is more worthwhile concerning the economic, environmental, and ecological benefits. Water hyacinth is one such lignocellulose biomass and, therefore, can be used as a suitable feedstock for cellulose nanofiber preparation. It has extremely high growth rates and is called the world's worst aquatic weed due to its ability to rapidly cover whole waterways. It also reproduces both asexually, through stolons, and sexually through seeds, which is difficult to control, and the seed can remain suspended for up to 20 years [10]. In most countries, water hyacinth is recognized as a major threat to agriculture and aquatic ecosystems because of its rapid growth rate [11]. This aquatic plant pollutes the environment and causes significant economic losses. A single water hyacinth plant may produce 140 million daughter plants per year, enough to cover an area of 1.40 km^2 with 28,000 tons of fresh biomass [12]. Native ecosystems have been harmed by this invasive species, which has blocked lakes and rivers [13]. Millions of dollars are being invested around the world to selectively eradicate the weed. The weed has high fiber content and no significant changes in cellulose content between the shoot and root [14]. Harvesting the plant biomass from water bodies and turning it into marketable commodities that could produce a profit is one way to lessen the detrimental effect of water hyacinth on aquatic ecosystems and agricultural crops.

Recycled paper is paper that has been reconstituted into paper again. The utilization of recycled paper as a source of raw material for new goods is important for both economic and environmental reasons. For the paper industry, recycled paper can be used as a primary or secondary source of raw material [15]. However, papers produced from recycled fibers have inferior resistance properties compared to papers with virgin fibers. Recycled fibers are morphologically different from virgin fibers, with a shorter average length, less flexibility, and a lower capacity to form interfiber bonds. These characteristics reduce the quality of the recycled paper. The use of nanofibrillated cellulose as a reinforcing agent in recycled paper enables the development of innovative nanostructured products with improved mechanical qualities. Cellulose nanofibers promote bonding and can be utilized in paper and board products as a strength enhancer [16]. Papers produced from nanofibrillated cellulose present higher density and flexibility, are optically transparent, have low porosity, and show excellent barrier properties to oxygen [17]. The inclusion of CNFs in papers boosts cellulose fiber contact and promotes better rearrangement, filling the empty spaces between the fibers during paper manufacture and resulting in a more uniform and compact structure. Therefore, the aim of the present study was twofold. Firstly, it attempted to prepare cellulose nanofibers for recycled paper reinforcement using a low-cost, ecologically friendly domestic blender. Secondly, the current research tries to reduce the harmful effects of water hyacinth on ecosystems by transforming it into a nanomaterial that might be used for reinforcement.

Experimental section

Materials

Water hyacinth stems as sources of cellulose were collected from the surrounding lake and the extraction process was done in the laboratory. The reagents and chemicals used in this study were toluene (99%), ethanol (97%), sodium hydroxide (97%), sodium hypochlorite, distilled water, acetic acid (99.5%), and KBr. All chemicals and reagents were used as received, without further purification.

Isolation of cellulose from water hyacinth

The raw water hyacinth (WH) sample was collected from Lake Tana. To isolate and purify cellulose from water hyacinth, the raw sample was passed through different pretreatment steps. For the elimination of contaminants and sample homogenization, basic pretreatments such as size reduction, extraction of soluble components, alkaline treatment, and bleaching were used in this work. First, water hyacinth stems were separated from their leaves and roots using a laboratory knife and allowed to dry in the sun for 7 days. Next, the collected stems were washed with distilled water to remove dust and then dried in an oven at a temperature of 60 °C for 24 h. The dried sample was chopped, milled, and sieved using a 1 mm sieve to get the powder form of the sample. Then, the obtained powder was sealed in a plastic (polyethylene) bag until used. Then 20 g of WH powder was dewaxed with a mixture of toluene and ethanol solvents with a ratio of 2:1 (v/v) [18]. The de-waxing process was conducted at 85 °C for 5 h to remove extractive components such as wax, pectin, and oils. The de-waxed powder was washed with distilled water and ethanol repeatedly and filtered using a sieve to remove the solvent. Alkaline pretreatment was used to reduce amorphous content, mainly hemicellulose, and to improve the nanocellulose production process. The

dewaxed sample was treated twice with 4% (wt/wt) NaOH solutions at 80 °C for 2 h. The ratio of the dewaxed sample to the NaOH solution used for alkaline treatment was 1:20 (g/ml) [19]. The treated sample was washed with diluted acetic acid and distilled water to neutral pH after each treatment. WH changed color from gray to white-brown during this procedure, as shown in Fig. 1, after which the suspension was allowed to settle overnight and the sediment recovered was employed in the subsequent treatments.

After alkaline treatment, the sample was bleached with a 4:1 (v/v) mixture of 5% (w/w) sodium hypochlorite (NaOCl) solutions and acetic acid under acidic conditions at pH 4 [20]. The ratio of the sample to the solvent used was 1:20 (g/ml). The process was performed at 80 °C for 2 h under constant agitation to remove lignin. Then, it was washed repeatedly with a diluted solution of sodium hydroxide and distilled water until free from acid and to achieve neutral pH until the white cellulose was obtained. Finally, the cellulose material was diluted to form a 1 wt% slurry for the subsequent processing stage.

Preparation of cellulose nanofibers

A simple, high-speed commercial blender was used to disintegrate cellulose into cellulose nanofibers. Before mechanical treatment, the chemically treated sample was diluted to 1 wt% fiber content in an aqueous solution. The sample was then put through a commercial blender for an hour to break down the microfiber into cellulose nanofibers, resulting in a homogeneous nanofiber dispersion in water (Fig. 1).

Waste paper recycling

Collection was the first phase in the paper recycling process. Waste paper of comparable quality was gathered since they could have equal amounts of fiber that can be recovered from the pulp. Collection, disintegration, deinking, washing, refining, pressing, and drying are all part of a whole recycling procedure. The paper was shredded after collection and chopped into little bits. Hot water was added to the finely shredded material, along with other chemicals like sodium hydroxide, to break down and separate the paper fibers. To eliminate ink and other contaminants, sodium hypochlorite was used.

Cellulose nanofibers (CNFs) reinforced recycled paper (RP) production

As shown in Fig. 2, CNF-reinforced RP composite paper sheets were prepared as follows: First, the pulp slurry prepared from the waste paper was dried, weighed, dissolved in hot water at 80 °C, and homogenized with a blender. After homogenization of the pulp in water, an aqueous suspension of cellulose nanofibers at different weight ratios (0, 1, 3, 5, 10, and 15 wt%) was added to the solution in order to produce composite papers. The ratio of CNFs to recycled papers is summarized in Table 1. To improve the homogeneous dispersibility of the cellulose nanofibers in the recycled papers, the mixtures were blended using a domestic blender, and then each mixture was transferred into a paper mold to form a paper sheet, which was then pressed to remove excess water and give the paper extra smoothness and strength. Finally, these paper sheets were allowed to dry in the sun for two days, and the composites containing nanofibers were

Fig. 1 Schematic representation of cellulose isolation and CNFs preparation from water hyacinth

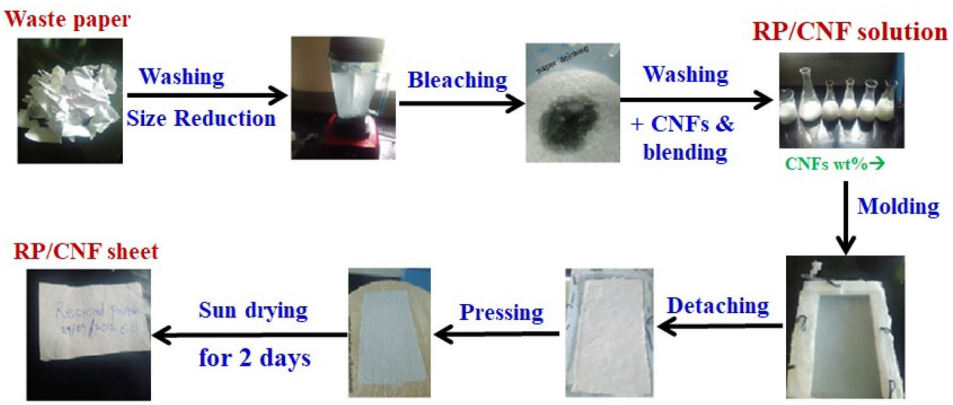

Fig. 2 Preparation scheme for CNFs reinforced recycled paper

coded according to their cellulose nanofiber content on a weight basis.

Characterization

The chemical composition of water hyacinth was determined. To do so, an air-dried WH sample of approximately 1 g (Wo) was boiled four times with a mixture of ethanol and toluene for 15 min each, washed thoroughly with distilled water, and then kept in the oven at 40 °C for 24 h. The dry sample was weighed and taken as an A fraction and then treated with 4% NaOH for 2 h at 80 °C, washed thoroughly with distilled water, dried at 50 °C for 24 h, and the dry weight was taken as the B fraction. The sample was again treated with a mixture of 5% (w/w) sodium hypochlorite solutions and acetic acid with a ratio of 4:1 (v/v) under acidic conditions at a pH of 4. The process was performed at 80 °C for 2 h under constant agitation to remove lignin. Then, it was washed repeatedly with a diluted solution of sodium hydroxide and distilled water until free from acid and to achieve a neutral pH. The sample was then dried at 80 °C for 24 h in the oven, and the dry weight was considered the C fraction. The lignocellulose substrates were then calculated as follows:

FTIR analysis was performed to characterize the chemical structure of raw water hyacinth and extracted cellulose and to study the physical interaction between CNFs and recycled papers in the composite sheet. FT-IR spectra were recorded using a Fourier-transform infrared spectrometer (FTIR-6600 Jasco, Japan). Recycled paper with 0 and 10 wt% CNFs, raw WH, and CNFs samples were dried in an oven at 50 °C for 2 h and then ground with potassium bromide in an agate mortar. The powders were then pressed into thin pellets and dried in an infrared box before being tested. These pellet samples produced FT-IR spectra in the wavenumber range of 400–4000 cm^{-1}. To describe the degree of fibrillation of cellulose after mechanical treatment; the optical property of cellulose nanofiber dispersion was measured using UV–Vis spectroscopy (Agilent-Technology, Chary60 UV–Vis).

Recycled papers have poor moisture resistance, and in this test, the water retention capacity of the composite paper sheet was tested. The water retention value (WRV) test provides information about composite paper's ability to take up water and swell. The test was carried out by weighting dried samples, and then the samples were rinsed in distilled water for a certain period of time. Next, the amount of water retained by each sample was determined by weighting the sample. The sample was weighted every 1 min using an analytical balance, and then WRV could be calculated by the equation: $WRV = \frac{W_{wet-W_{dry}}}{W_{dry}} x100$, Where: W_{wet} and W_{dry} are the wet and dry sample weights, respectively [21]. Density is an important physical property of a material that should be considered in composite materials. In order to measure the density of composites, the volume (cm^3) and mass (g) of each paper sheet were carefully measured, and the ratio of mass to volume was reported. For data accuracy, five specimens were measured for each composite sample, and the average values were considered.

Tensile testing data were collected to measure the mechanical performance of the composite papers using a tensile testing instrument (Tensile Strength Tester, Model: H5KS) which corresponds to the ratio between the force and the area of the sample, expressed in N/m^2. The elongation percentage of each sample was calculated by the ratio between the change in length and the initial length of the

Table 1 Ratio of paper and CNFs in wt (%) and in (g)

Recycled Pulp	Recycled fiber		Nanofibrillated cellulose(CNFs)	
	Wt (g)	Wt (%)	Wt (g)	Wt (%)
Writing/Printing Paper	4	100	0	0
	3.96	99	0.04	1
	3.88	97	0.12	3
	3.8	90	0.2	5
	3.6	95	0.4	10
	3.4	85	0.6	15

Table 2 Water hyacinth percentage composition determination

Cellulose (%)	Hemicellulose (%)	Lignin (%)
$= \frac{C}{W_o} x100$	$= \frac{A-B}{W_o} x100$	$= \frac{B-C}{W_o} x100$

sample expressed in percent. The thermal stability of the neat and composite samples was analyzed. Using N_2 gas, the measurements were made with a thermogravimetric analyzer (HCT-1 Beijing Henven instrument, China) with a temperature range of 50 to 600 °C and a heating rate of 10 °C/min. A sample weight of 11 ± 0.015–12 ± 0.013 mg was used to take the measurements. Data on weight percent as a function of temperature and the rate of weight loss as a function of temperature were recorded.

Results and discussion

Chemical composition of water hyacinth

The chemical composition of the WH stem was determined by following a similar procedure to cellulose isolation except that drying and weighing of a sample in each chemical treatment were conducted. As it was determined based on the formula in Table 2, the composition values were 55% cellulose, 19% hemicellulose, 12% (fat, oil, wax, and pectin), and 14% lignin. As demonstrated in Table 3, these values were compared with previously reported data.

The cellulose, hemicellulose, and lignin contents of WH obtained in this study are almost within the ranges of previous studies. The variations in the composition of WH among the different studies might be attributed to the cultivation period, growing environment, differences in spices, etc. The lignin content of WH was considerably lower than other lignocellulose materials like hardwood stems (18–25%), pineapple leaf (25–29%), and sugar cane bagasse (20–22%) [28, 29]. In general, the significantly higher cellulose content of WH evaluated in this study inspired the research team to find an application for a double benefit, namely, decreasing invasive plant expansion and using it as reinforcement.

Characterizations of water hyacinth cellulose nanofibers

The isolated cellulose from water hyacinth through chemical treatments was subjected to a domestic blender. Cellulose is poorly water-soluble due to the strong hydrogen bonds, and that limits its processability and application. Hence, it is usually converted into nanoforms. Mechanical treatments such as grinding, high-pressure water jet systems, ultrasonication, etc. are employed to disintegrate cellulose chains into cellulose nanofibers. In this study, a very simple and cost-effective domestic blender was used for mechanical disintegration. As can be seen in the preparation scheme of cellulose nanofibers from water hyacinth (Fig. 1), the water dispersibility of cellulose at 1 wt% concentration was remarkably enhanced after the domestic blender treatment. Non-mechanically treated cellulose settles immediately, whereas the same concentration of mechanically treated cellulose stays as a homogenous dispersion for a long period of time. This shows that the hydrogen bond networks are broken via mechanical force and water molecules can easily penetrate the cellulose surface. Moreover, the long-time homogenous dispersibility of cellulose in water indicates the disintegration of cellulose chains into cellulose nanofibers.

FTIR characterization of raw WH and extracted cellulose

The FTIR spectra of water hyacinth and extracted cellulose are shown in Fig. 3. The characteristic peaks for raw WH and extracted cellulose were observed in the range of 3500–3000 cm^{-1}, which corresponds to the stretching of OH due to hydrogen bond interaction with hydroxyl groups [30, 31]. The spectra associated with C-H stretching appeared in both samples in the wavenumber range of 3000–2800 cm^{-1}. This indicates that all samples have aliphatic saturated components [32]. The acetyl and uronic ester linkages of the carboxylic groups of the ferulic and p-coumaric acids of lignin and hemicelluloses demonstrated a peak at 1735 cm^{-1} [33]. This peak disappeared in the extracted cellulose after the chemical treatment, which indicates the effective removal of lignin and hemicellulose. Both samples showed the band at around 1639 cm^{-1}, corresponding to the vibration of water molecules absorbed [34]. Lignin's aromatic ring vibration occurs in the 1500–1200 cm^{-1} range [35]. The characteristic peak appeared at 1248 cm^{-1} in untreated fiber but not in the pure cellulose fiber, indicating that the chemical treatment successfully removed the lignin component. Raw WH and extracted cellulose showed a characteristic peak at 1426 cm^{-1} due to CH_2 in-plane bending. In the wavenumber range from 1030–1070 cm^{-1}, both samples displayed a characteristic peak

Table 3 Chemical composition of water hyacinth from different studies

Constituent (%)	[22]	[13]	[23]	[24]	[25]	[26]	[27]	This study
Cellulose	34.19	23.31	35	66.9	60	24.15	31.81	55
Hemicellulose	17.66	22.11	33	23	23.7	27.33	25.64	19
Lignin	12.22	12.58	15.5	9.5	13	12.39	3.55	14

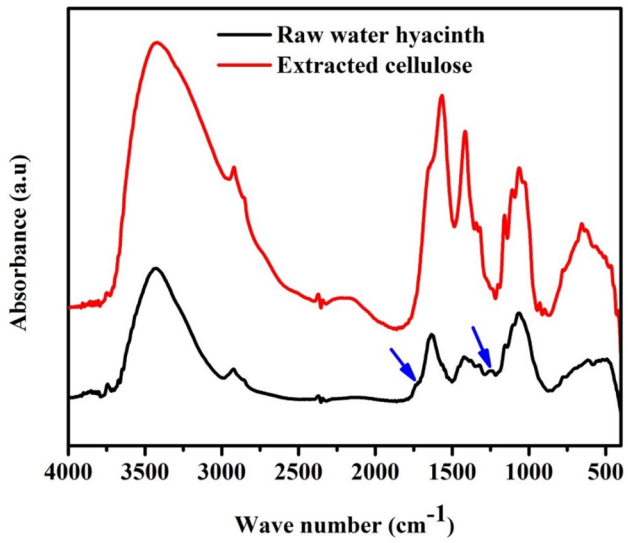

Fig. 3 FTIR spectra of raw water hyacinth and extracted cellulose

due to the stretching of C–O–C of the pyranose ring in cellulose [25, 36].

Optical properties of cellulose nanofibers (CNFs)

Figure 4 shows the light transmittance of a 1 wt% water dispersion of raw water hyacinth, cellulose, and cellulose nanofibers. The light transmittance of the cellulose fiber dispersion is strongly associated with the fibers' thickness and water dispersibility. For raw water hyacinth and pure cellulose, it is hard to take the light transmittance data of the dispersion since the solid component immediately settles at the bottom of the cuvette. On the other hand, CNF dispersion showed significant transparency, particularly at higher wavelengths. This implies that CNFs were much thinner than the wavelength of visible light as compared with raw WH and cellulose. The size and shape of the material are heavily linked to transparency. To put it another way, if a material has a rough surface and a large size, it will have less transmittance due to light extinction caused by the scattering and absorption of incoming radiation. This is why raw WH and cellulose have lower transmittance than cellulose nanofiber. Generally, from this UV–Vis data, it can be concluded that the mechanical treatment through a domestic blender was effective in converting the aggregated cellulose chains into shorter and thinner fibers, which resulted in good transparency and homogenous water dispersibility.

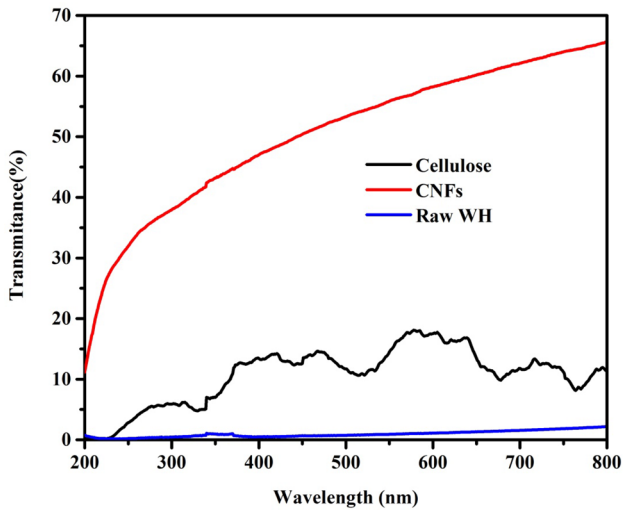

Fig. 4 UV–Vis transmittance of 1 wt% dispersion of raw WH, cellulose and CNFs

Characterizations of CNFs reinforced composite paper

Figure 5 shows a photo of composite papers with an increasing weight percent of CNFs in the upward direction. As it can be seen there, as the filler content increased, the composite paper decreased in both length and width. Moreover, the thickness measurement results also revealed that increasing the CNF content reduced the thickness values of the composite paper in the same order. The thickness values for the composite papers containing 0, 1, 3, 5, 10, and 15% CNFs were 1.274 ± 0.020, 1.086 ± 0.011, 0.976 ± 0.032, 0.956 ± 0.041, 0.884 ± 0.032, and 0.8 ± 0.012 mm, respectively. The reduction in thickness, length, and width had a

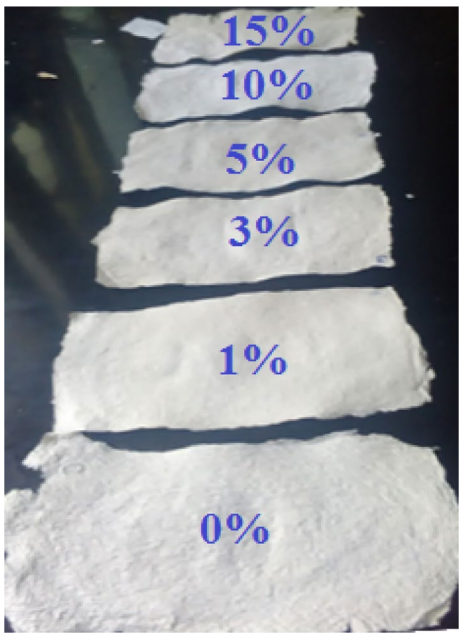

Fig. 5 The neat recycled paper having no CNFs (0%) and the RP/CNFs composite paper containing 1, 3, 5, 10, and 15% CNFs

direct contribution to the increment in paper sheet density. In the previous study, it was also reported that the addition of CNF to sheets remarkably increased the paper sheet's density [37]. The possible reasons for the paper sheet's density increment upon the addition of CNF as reinforcement might be one: the CNF will reduce the radius of the water meniscuses formed during the dewatering of the sheet, thus increasing the pressure difference between the water phase and surroundings, which helps consolidate a sheet by pressing fibers into close contact. Secondly, CNFs might be attached to the fiber surfaces as a layer and help strengthen and increase the contact area, thus increasing the number of hydrogen bonds. This is associated with an improvement in the permanent formation of linkages where fibers have come into contact during wet pressing. Surface roughness, on the other hand, is an unfavorable characteristic of recycled paper. As shown in Fig. 5, the addition of CNFs as filler greatly smoothed the rough surface, with the effect becoming more pronounced as the amount of CNFs increased. CNFs are thought to fill the gaps created by fiber–fiber crossings or pores found between the fibers of recycled paper. This is due to the reactive hydroxyl groups on the CNF surface's ability to develop strong interactions with recycled cellulose fibers during the papermaking process, allowing for improved rearrangement and filling of the empty spaces between the fibers.

FTIR characterization of CNFs, RP and RP-CNFs (10%)

The FTIR spectra of cellulose nanofibers (CNFs), recycled paper (RP), and recycled paper with 10% CNFs (RP-CNFs (10%)) are shown in Fig. 6. The FTIR spectra of RP, CNFs, and RP-CNFs composites were similar due to structural similarities. However, compared to the filler and matrix peaks, the strength of the peak at around 3410 cm^{-1}, which corresponds to the OH groups, was dramatically reduced in the spectrum of the RP-CNFs composite. This shows that including cellulose nanofibers into the paper matrix results in considerable interactions with the recycled paper matrix, limiting the OH group's mobility in the composite paper sheet. In general, the composite sheets' low intensity and narrow peaks are signs of interactions between the matrix and fillers. Reactive OH is found in cellulose nanofibers.

Water absorption test

Water absorption capacities of recycled paper and CNF composite sheets were investigated, and six paper sheets were compared. Figure 7 depicts the overall trend of sheet water absorption. With a rise in the weight percent of cellulose

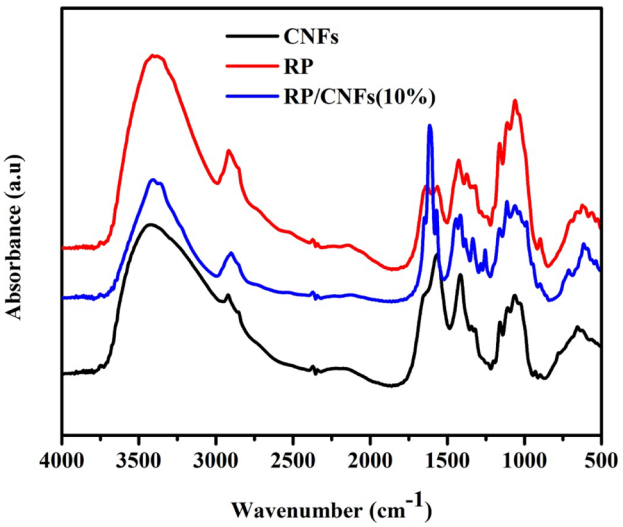

Fig. 6 FTIR spectra of cellulose nanofibers, recycled and composite papers

nanofibers in the composites, the water holding capacity of paper sheets tends to decrease. Figure 7 shows a significant difference in swelling between sheets having up to 3 wt% CNFs and those containing 5, 10, and 15 wt% CNFs. The neat recycled paper sheet absorbs the most moisture, showing that it has more porosity than papers with CNF fillings. The difficulty of water molecules accessing the dense network formed by recycled paper and cellulose nanofibers through hydrogen bonding explains why composite sheets have the lowest water holding capacity. The paper sheet with the highest moisture resistance had 10% CNFs, indicating that this concentration was appropriate to robust interaction with fibers in the recycled paper sheet. The aggregation of CNFs at higher concentrations generates an uneven

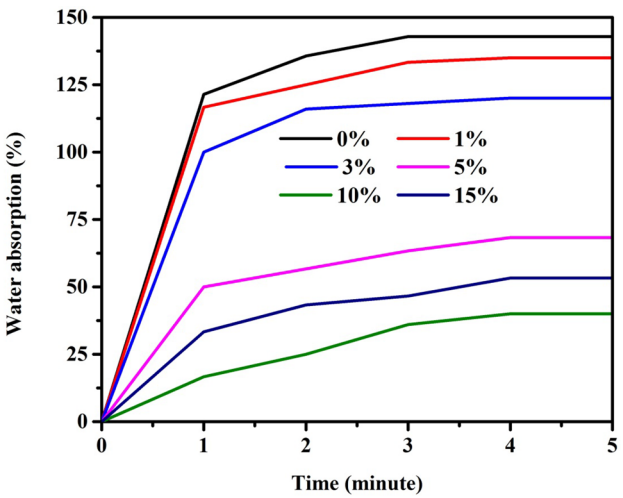

Fig. 7 Swelling behavior of neat RP and RP-CNFs composite sheets in distilled water

distribution in the recycled paper matrix, which might lead to poor interfacial interaction between the matrix and filler, lowering the moisture resistance of paper sheets containing 15 wt% CNFs. Generally, from this test, it can be concluded that the limited application of recycled papers due to high water sensitivity was significantly improved with the inclusion of cellulose nanofibers as reinforcement.

Tensile testing

To examine the reinforcement effect of CNFs, the tensile properties of the neat RP sheet and RP/CNFs composite sheets were measured using a tensile machine, which corresponds to the ratio between the force and the area of the sample, expressed in N/m^2. Three replicates were considered for each sample. The representative stress–strain curves for the neat RP sheet and RP/CNF composite sheets at different weight percent of CNFs are indicated in Fig. 8. The percent elongation of each sample was calculated by the ratio between the change in length and the initial length of the sample expressed in percent. The thicknesses of the recycled paper sheets range from 1.274 ± 0.020 mm for 0 to 0.8 ± 0.012 mm for 15 wt% CNF containing recycled paper sheets. The presence of CNFs in the recycled paper sheets promotes a better rearrangement, filling the empty spaces between the fibers during the production of the paper and providing a more uniform, compact, and dense structure [38]. The density of recycled paper sheets increased from 16.9 ± 0.034 g/cm^3 for 0 to 27.8 ± 0.046 g/cm^3 for 10 wt% CNF containing composite papers. The increase in density and, as a result, the reduction in porosity of paper sheets is critical since these factors are linked to improved mechanical performance. The larger contact area between adjacent cellulose fibers allows for more hydrogen bridge connections to form, resulting in a denser network and increased paper strength and stiffness. On the other hand, the % elongation of the recycled paper shows increments with increasing the concentration of CNF from 2.4 ± 0.021% for the neat recycled paper to 11.0 ± 0.051% for a 10 wt% CNF containing paper sheet, but it shows a sudden decrease to 9.4 ± 0.025% upon the addition of 15 wt% CNFs. This indicates that the addition of cellulose nanofibers above 10 wt% makes the paper stiffer and harder, which leads it to easily create cracks and result in poor ductility. The tensile strength of RP/CNF composite paper sheets also sharply increased with increasing the CNF content from 39.1 ± 0.067 kPa for 0 to 52.2 ± 0.027 kPa for 10 wt% CNF-containing recycled paper sheets. The improvement in tensile strength may be attributed to the percolation between the RP matrix and the CNFs through hydrogen bonding and hydrophobic interactions, which promote the formation of rigid interconnected structures to resist the tensile stress. However, at 15 wt% CNF inclusion, a decrease in tensile strength was observed. The reason might be associated with the aggregation of CNFs at a higher concentration, which causes poor interaction with the recycled paper matrix. Previous research results supported this finding. In the study, the mechanical strength of epoxy resin was significantly improved upon the inclusion of iron-carbon nanotubes (Fe-CNTs) filler up to 4 wt% and showed decline above this concentration [39]. Other study also demonstrated that above the threshold concentration reinforcements have negative effects on the mechanical strength of the composite materials [40, 41]. This is supported by the water absorption test, which demonstrated that water molecules could easily penetrate the RP structure at 15 wt% CNF inclusion due to weak intra- and intermolecular hydrogen bonding interactions when compared to 10 wt% CNF containing a composite sheet.

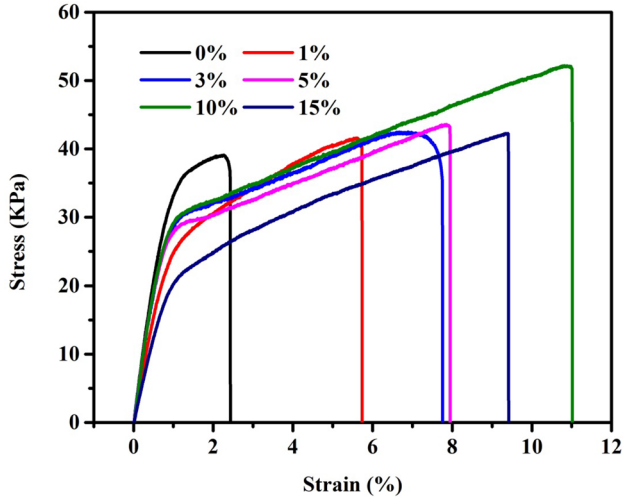

Fig. 8 Representative stress–strain curves for the neat RP and RP/CNFs composite sheets

Thermal properties of the neat RP and PR-CNFs composite papers

Figure 9 shows the TGA and DTGA curves of neat RP and RP-CNF composite papers with various CNF contents. At around 90 °C, almost all samples showed a loss in mass, which was corresponding to the evaporation of water from the paper sheets. The thermal stability of each sample was compared by considering temperature values at 10% and 50% mass losses and the remnant masses at 600 °C. The neat recycled paper (RP) lost 10% of its mass at 190 °C. However, the incorporation of CNFs into the composite enhanced the temperature by 10% mass losses, and the temperature values were 191, 194, 192, 200, and 201 °C for 1, 3, 5, 10, and 15 wt% CNF-containing composites, respectively. Similarly, the neat RP showed 50% mass loss at a lower temperature of 213 °C, and the incorporation of

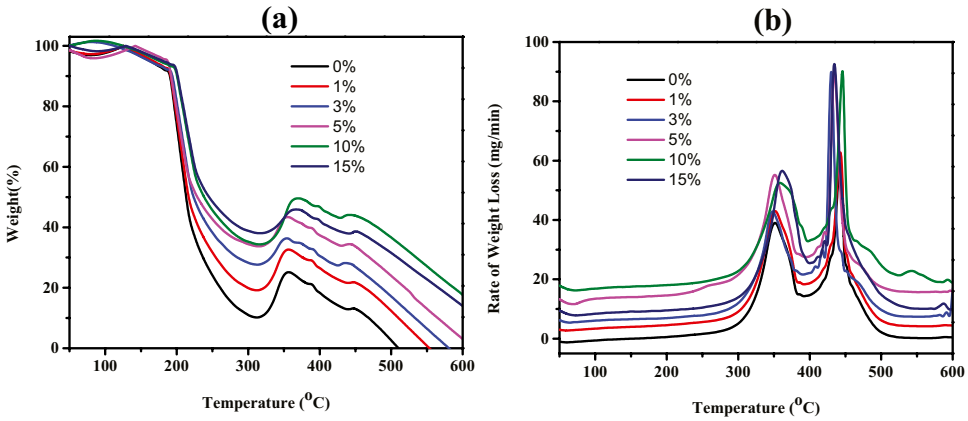

Fig. 9 TGA (**a**) and DTGA (**b**) curves for neat RP composite papers with various CNFs contents

CNFs increased the temperature to 217, 224, 227, 238, and 245 °C for 1, 3, 5, 10, and 15 wt% CNF-containing composite papers, respectively. Based on these TGA results, it is possible to conclude that the addition of CNFs as reinforcement significantly improved the thermal stability of recycled papers. As the CNF content increased, the thermal stability of the composites also increased. However, the 10 wt% CNFs seems to be the optimum concentration for enhancing the thermal stability of recycled papers. When the thermal stability of the composites was compared in terms of total mass loss temperature, the neat RP lost its total mass at 510 °C. On the other hand, 1 and 3 wt% CNF inclusion enhanced the total mass loss temperature to 553 and 580 °C, respectively. Higher CNF content containing composites, 5, 10, and 15 wt% had 3%, 18%, and 13% remnant masses at 600 °C, respectively. The DTGA curves (Fig. 9b) also showed that the degradation rate temperature of 5, 10, and 15 wt% CNF-containing composite papers was higher than the neat RP and other lower CNF-containing composite papers. The hydrogen bonds and hydrophobic interaction between the CNFs and the RP matrix played significant roles in the improved thermal degradation temperature of RP. The strength of hydrogen bonding interactions could be increased when the CNF content in the composite papers rose, and therefore the thermal stability of RP was greatly improved. The best combination of 10 wt% CNFs with recycled papers is owing to their improved miscibility with the RP matrix, which could be facilitated by hydrogen bonds.

Conclusion

In this study, water hyacinth was deliberately selected as the source of cellulose, after realizing its devastating effect on water bodies and aiming to convert it into some usable forms. The chemical composition of the water hyacinth used in the study was determined gravimetrically, and the highest percentage of it (55%) was cellulose. Through simple chemical treatments, cellulose could be extracted from water hyacinth. To increase its functionality and processability, the extracted cellulose was disintegrated into nanofibers using a high-performance domestic blender, which was both cost-effective and environmentally friendly. The FT-IR spectroscopic data showed that hemicellulose and lignin in water hyacinth were removed by alkaline and hypochlorite treatments, respectively. The light transmittance data via UV-Vis spectroscopy revealed that 1 wt% CNFs water dispersion showed good transparency (65% at 800 nm). In this study, the prepared CNFs were used as reinforcement fillers in recycled paper. The composite papers were characterized in terms of their chemical structure, water sensitivity, mechanical strength, and thermal stability. The FTIR spectral data of the composite materials revealed there were interactions between the CNF filler and the recycled paper matrix. The incorporation of CNFs into the recycled paper matrix significantly enhanced the thermo-mechanical properties of recycled papers. The ultimate tensile strength of the recycled paper linearly increased with increasing the concentration of CNFs and the maximum value (52.2±0.027 KPa) was obtained for 10 wt% CNF-containing composite recycled paper. The percent elongation values also increased with increasing nanofiller content up to 10 wt% and then decreased. This means that as the amount of CNF increased, the paper became stronger and deformed less. The low deformability of composites under tensile loads can be ascribed to a high level of adhesion between the matrix and cellulose nanofibers since the strong interactions between the fibers and matrix molecules do not allow the paper sheet to elongate. The TGA and DTGA data also revealed that CNFs have effectively increased the thermal stability of recycled paper. The high CNF content-containing composite papers showed better thermal stability. The water sensitivity of recycled paper was meaningfully improved with the addition of CNFs as reinforcing agents, and a lower percentage of water absorption was exhibited by higher concentrations of CNF-containing composite papers. From this, it can be concluded that the strong hydrogen bond network reduced

water molecules' entry into the interior part of the composite materials. The low moisture absorption and high percent elongation values obtained suggest that CNFs could be an effective reinforcing material for recycled paper. It was also shown that an increase in the content of nanofibers resulted in an increase in the densities of the composites. From the overall characterizations made in this study, it can be concluded that CNFs at 10 wt% could be the optimum concentration to reinforce recycled papers. Generally, this study has demonstrated that water hyacinth can serve as a good biomass feedstock for producing CNFs with a powerful application and alternative way of reducing the negative effects of water hyacinth on the environment through the effective utilization of CNFs as fillers in recycled paper.

Declarations

Conflict of interests The authors declare that they have no financial or other personal interests that could have appeared to influence the work reported in this paper.

References

1. Xue Y et al (2021) Zephyranthes-like Co2NiSe4 arrays grown on 3D porous carbon frame-work as electrodes for advanced supercapacitors and sodium-ion batteries. Nano Res 14(10):3598–3607
2. Kong Q et al (2017) Improving flame retardancy of IFR/PP composites through the synergistic effect of organic montmorillonite intercalation cobalt hydroxides modified by acidified chitosan. Appl Clay Sci 146:230–237
3. Yihun FA et al (2020) Highly transparent and flexible surface modified chitin nanofibers reinforced poly (methyl methacrylate) nanocomposites: Mechanical, thermal and optical studies. Polymer 197:122497
4. Samyn P, Barhoum A (2018) Engineered nanomaterials for papermaking industry. Fundamentals of Nanoparticles. Elsevier, pp 245–277
5. Sindhu KA, Prasanth R, Thakur VK (2014) Medical applications of cellulose and its derivatives: present and future. Nanocellulose polymer nanocomposites, pp 437–477
6. Xia Y et al (2003) One-dimensional nanostructures: synthesis, characterization, and applications. Adv Mater 15(5):353–389
7. Li D, Xia Y (2004) Electrospinning of nanofibers: reinventing the wheel? Adv Mater 16(14):1151–1170
8. Hubbe MA et al (2008) Cellulosic nanocomposites: a review. BioResources 3(3):929–980
9. Tejado A et al (2012) Energy requirements for the disintegration of cellulose fibers into cellulose nanofibers. Cellulose 19(3):831–842
10. Rezania S et al (2015) Perspectives of phytoremediation using water hyacinth for removal of heavy metals, organic and inorganic pollutants in wastewater. J Environ Manage 163:125–133
11. Harun M et al (2011) Effect of physical pretreatment on dilute acid hydrolysis of water hyacinth (Eichhornia crassipes). Biores Technol 102(8):5193–5199
12. Thi BTN et al (2017) Comparison of some pretreatment methods on cellulose recovery from water hyacinth (Eichhornia crassipe). J Clean Energy Technol 5(4):274–279
13. Xia A et al (2013) Enhancing enzymatic saccharification of water hyacinth through microwave heating with dilute acid pretreatment for biomass energy utilization. Energy 61:158–166
14. Chaosri P, Srihanam P (2020) Preparation and Characterization of Water Hyacinth Cellulose/Keratose Composite Films. Sci Technol Eng J (STEJ) 6(2):62–71
15. Dienes D, Egyhazi A, Reczey K (2004) Treatment of recycled fiber with Trichoderma cellulases. Ind Crops Prod 20(1):11–21
16. Balea A et al (2016) Effect of bleached eucalyptus and pine cellulose nanofibers on the physico-mechanical properties of cartonboard. BioResources 11(4):8123–8138
17. Fukuzumi H, Saito T, Isogai A (2013) Influence of TEMPO-oxidized cellulose nanofibril length on film properties. Carbohyd Polym 93(1):172–177
18. Jiang F, Hsieh Y-L (2015) Cellulose nanocrystal isolation from tomato peels and assembled nanofibers. Carbohyd Polym 122:60–68
19. Lee H, Hamid SBA, Zain S (2014) Conversion of lignocellulosic biomass to nanocellulose: structure and chemical process. The Sci World J
20. Kim D-Y et al (2016) Preparation of nanocellulose from a kenaf core using E-beam irradiation and acid hydrolysis. Cellulose 23(5):3039–3049
21. Fillat Ú et al (2018) Assessing cellulose nanofiber production from olive tree pruning residue. Carbohyd Polym 179:252–261
22. Ahn DJ, Kim SK, Yun HS (2012) Optimization of pretreatment and saccharification for the production of bioethanol from water hyacinth by Saccharomyces cerevisiae. Bioprocess Biosyst Eng 35(1):35–41
23. Ganguly A et al (2013) Enzymatic hydrolysis of water hyacinth biomass for the production of ethanol: optimization of driving parameters
24. Kumar A, Singh L, Ghosh S (2009) Bioconversion of lignocellulosic fraction of water-hyacinth (Eichhornia crassipes) hemicellulose acid hydrolysate to ethanol by Pichia stipitis. Biores Technol 100(13):3293–3297
25. Asrofi M et al (2018) Isolation of nanocellulose from water hyacinth fiber (WHF) produced via digester-sonication and its characterization. Fibers and Polymers 19(8):1618–1625
26. Feng L et al (2014) Combined severity during pretreatment chemical and temperature on the saccharification of wheat straw using acids and alkalis of differing strength. BioResources 9(1):24–38
27. Yan J et al (2015) Bioethanol production from sodium hydroxide/hydrogen peroxide-pretreated water hyacinth via simultaneous saccharification and fermentation with a newly isolated thermotolerant Kluyveromyces marxianu strain. Biores Technol 193:103–109
28. Dos Santos RM et al (2013) Cellulose nanocrystals from pineapple leaf, a new approach for the reuse of this agro-waste. Ind Crops Prod 50:707–714
29. Athinarayanan J, Alshatwi AA, Periasamy VS (2020) Biocompatibility analysis of Borassus flabellifer biomass-derived nanofibrillated cellulose. Carbohyd Polym 235:115961
30. Asrofi M et al (2017) XRD and FTIR studies of nanocrystalline cellulose from water hyacinth (Eichornia crassipes) fiber. In Journal of Metastable and Nanocrystalline Materials. Trans Tech Publ
31. Abraham E et al (2011) Extraction of nanocellulose fibrils from lignocellulosic fibres: A novel approach. Carbohyd Polym 86(4):1468–1475
32. Lani NS et al (2014) Isolation, Characterization, and Application of Nanocellulose from Oil Palm Empty Fruit Bunch Fiber as Nanocomposites. J Nanomater 2014:702538
33. Cherian BM et al (2008) A Novel Method for the Synthesis of Cellulose Nanofibril Whiskers from Banana Fibers and Characterization. J Agric Food Chem 56(14):5617–5627
34. Poletto M et al (2011) Crystalline properties and decomposition kinetics of cellulose fibers in wood pulp obtained by two pulping processes. Polym Degrad Stab 96(4):679–685

35. Onyianta AJ, Dorris M, Williams RL (2018) Aqueous morpholine pre-treatment in cellulose nanofibril (CNF) production: comparison with carboxymethylation and TEMPO oxidisation pre-treatment methods. Cellulose 25(2):1047–1064
36. Xu F et al (2013) Qualitative and quantitative analysis of lignocellulosic biomass using infrared techniques: a mini-review. Appl Energy 104:801–809
37. Eriksen Ø, Syverud K, Gregersen Ø (2008) The use of microfibrillated cellulose produced from kraft pulp as strength enhancer in TMP paper. Nord Pulp Pap Res J 23(3):299–304
38. Dufresne A (2017) Nanocellulose: from nature to high performance tailored materials. Walter de Gruyter GmbH & Co KG
39. Zhang J, Kong Q, Wang D-Y (2018) Simultaneously improving the fire safety and mechanical properties of epoxy resin with Fe-CNTs via large-scale preparation. J Mater Chem A 6(15):6376–6386
40. Kong Q et al (2022) Influence of multiply modified FeCu-montmorillonite on fire safety and mechanical performances of epoxy resin nanocomposites. Thermochim Acta 707:179112
41. Yihun FA et al (2021) Thermo-mechanically improved polyvinyl alcohol composite films using maleated chitin nanofibers as nano-reinforcement. Cellulose 28(5):2965–2980